

Infrasonic Detection of Tornadoes and Tornadic Storms

Summary

There is evidence that infrasonic observing systems have significant potential to improve tornado warnings. A key section 8 in this background paper summarizes six case studies, describing infrasonic detection of tornadoes, tornadic storms, and funnels under various conditions and summarizing warning times. The near infrasound systems applied in this research provide a new way of “hearing” low-frequency sounds in the atmosphere and focus on a different, higher frequency window than historical infrasonic research dating to the 1970’s. The purposes of this paper are to provide background and a status report on this tool for tornado detection. This technology is at an ideal point for demonstration in an operational context.

Table of Contents by Section

1. What is infrasound?	P3
2. What sensors and techniques are required for the detection of these low-level, low frequency sounds?	P4
3. At what distances from a source can infrasound be detected?	P6
4. But hasn't the use of infrasound for monitoring severe weather been researched since the 1970's with no operational uses resulting?	P6
5. A Typical Infrasonic Summer Day	P7
6. A contrast to the quiet summer day	P11
7. How can vortices generate sound?	P13
8. Case studies of infrasound associated with tornadoes and tornadic storms	P14
9. But are there regional signals that can cause false alarms?	P19
10. How can Infrasonic Observatories Improve Tornado Warnings?	P20
11. What are the next steps?	P21
12. What form will the prototype network take? -and- What steps will be critical to assessment?	P21
13. What are the Anticipated Benefits-to-Cost Ratios?	P24
14. References	P25

Infrasonic Detection of Tornadoes

1. What is infrasound?

Infrasound is the range of acoustic frequencies below the audible (Bedard and Georges, 2000). For a typical person this is at frequencies below about 20 Hz, where the threshold of human hearing and feeling crossover. There is a rational analog between sound and the relationship of infrared to visible light. Thus, one can call the frequency range 1 to 20 Hz near infrasound and the range from about .05 to 1 Hz infrasound. Below about .05 Hz where gravity becomes important for propagation, atmospheric waves are usually called acoustic/gravity waves. Figure 1 indicates the sound pressure levels as a function of frequency with the threshold of human hearing as a reference. A frequency of 1 Hz is eight octaves below middle C. The lowest frequency on a piano keyboard is A at 27.5 Hz, consistent with being near the lowest limits of a typical persons hearing. Acousticians have adopted the convention of defining sound levels relative to the threshold of human hearing, and most situations involve the perceptions of people to sound. However, the infrasonic signal data can be quite valuable and provide information on a range of geophysical processes. More background on infrasonics may be found on the web site <http://www.etl.noaa/et1/infrasound/>.

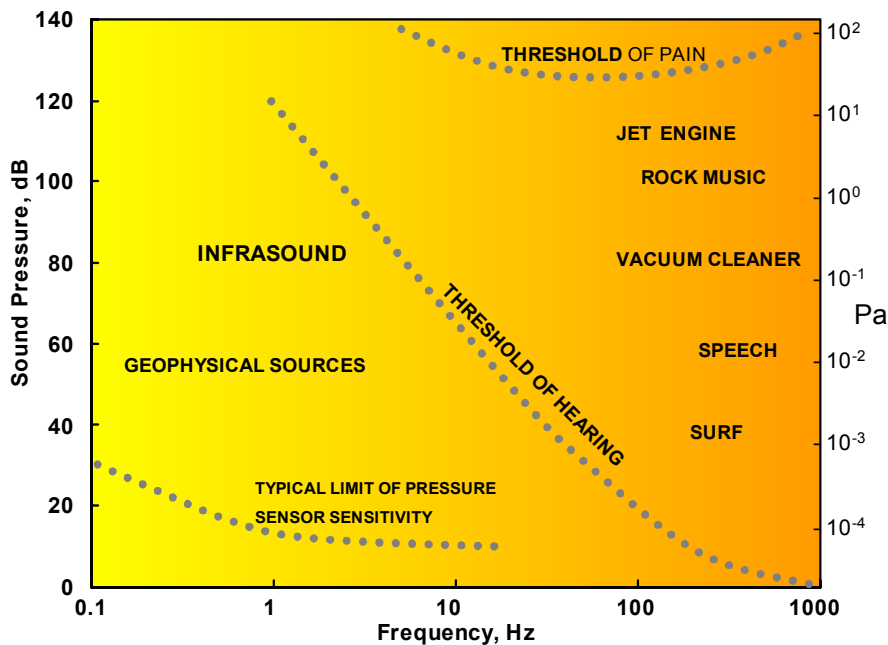


Fig 1 Sound pressure amplitude as a function of frequency compared with the threshold of human hearing at lower frequencies

2. What sensors and techniques are required for the detection of these low-level, low frequency sounds?

A critical need was the development of an effective method for reducing noise from large but highly spatially incoherent pressure fluctuations, while still detecting infrasonic signals. Daniels (1959) made the critical breakthrough in devising a noise reducing line microphone. His concept was to match the impedance along a pneumatic transmission line using distributed input ports and pipe size changes to minimize attenuation. This innovation exploiting the high spatial coherence of infrasound and the small spatial coherence of pressure changes related to turbulence, provided signal-to-noise ratio improvements of the order of 20 dB. Variations of his concept are currently in use worldwide. Figure 2 is a photo of a spatial filter using 12 radial arms with ports at one-foot intervals and covering a diameter of fifty feet. We have adapted porous irrigation hose for use as a distributed pressure signal transmission line (an infrasonic noise reducer), saving considerable costs in fabrication and maintenance. The present wind noise reducers can look a lot like an octopus (with four extra arms) with black porous hoses radiating outward from a central sensor.

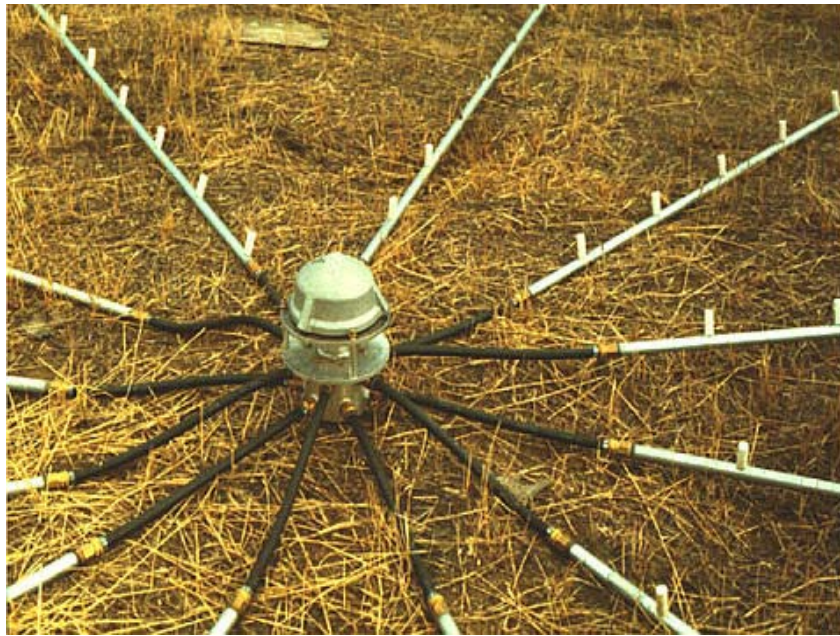


Figure 2. Photograph of a spatial filter for reducing wind-induced pressure fluctuations in the infrasonic frequency range.

A reasonable assumption, for sound waves from point sources after traveling paths of tens or hundreds of wavelengths, is that the wave fronts are planar. This model is usually used in processing data from infrasonic observing systems and was the basis for the design of beamsteering algorithms developed to determine correlation coefficient, azimuth, and horizontal

phase speed. Effective separations for microphones in arrays are usually about $\frac{1}{4}$ of the primary acoustic wavelength to be detected. In addition, the fact that infrasonic signals show little change with distance is the basis of the method for the reduction of unwanted pressure noise. Figure 3 shows a typical array layout. Usually an infrasonic observatory consists of 4 sensors equipped with spatial filters in a rough square configuration. The twelve porous hoses are often 50-feet in length and bent back toward the center so that the complete filter covers a diameter of about 50 feet. These noise reducers can operate in rain and snow without affecting infrasonic signals. Vegetation can reduce wind in the lower boundary layer and further improve wind noise reduction.

Array Geometry

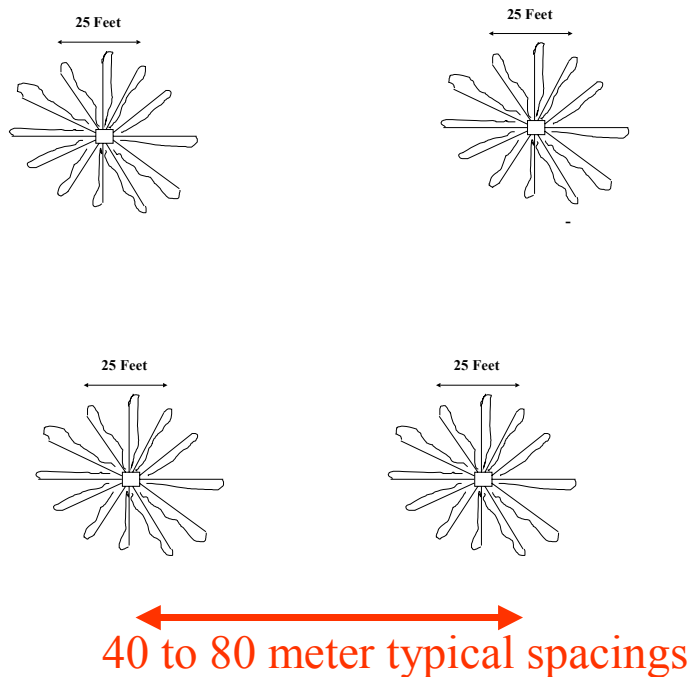


Figure 3. View of a typical infrasonic observatory array configuration. The exact positioning of the twelve porous irrigation hoses radiating outward from each of the four sensors is not critical.

Conventional microphones being designed for audio frequencies do not respond to infrasonic frequencies. There are a number of reasons for this, in addition to the fact that there was no practical need to detect inaudible sounds. For example, extended low frequency sensitivity could cause undesirable dynamic response limitations. Thus, a microphone having a diaphragm deflecting in response to sound waves typically has a leakage path to a reference volume behind the membrane. This permits frequencies below the cutoff of such a high pass filter to appear on both sides of the sensor, canceling response. We use sensitive differential pressure sensors integrated with a large, well-defined reference volume and calibrated flow resistor providing a stable high-pass filter time constant. The volume is insulated to create a stable temperature environment. These sensors are rugged, relatively small (less than 2x2x2 feet), and relatively light (about 22 pounds). We typically operate for years with few problems. Because arrays of

sensors are applied to detect and process signals, there is a need to match the microphone sensitivities and phase characteristics. This required the creation of a family of static and dynamic pressure calibration techniques, as well as methods for measuring flow resistance. The infrasonic sensors are carefully matched and interchangeable.

3. At what distances from a source can infrasound be detected?

Cook (1962) has shown how unimportant molecular attenuation is to infrasonic propagation (5×10^{-8} dB per km), whereas sound at 2 kHz will attenuate at 5 dB per km. Since infrasound below 1Hz is virtually unattenuated by atmospheric absorption, it is detectable at distances of thousands of kilometers from the source. Thus, an infrasonic wave at a frequency lower than 1Hz will travel for 1000 kilometers with less attenuation than a sound wave at 2 kHz traveling for 1000 feet. Temperature changes in the atmosphere affect infrasound in the same way that light waves are refracted by lenses. In addition, wind speed changes contribute to sound refraction, guiding sound waves as they travel for long distances. Some waves escape and travel upwards to great heights in the ionosphere where they dissipate, while other sound rays are trapped and bounce back and forth many times between the earth's surface and the upper atmosphere as they travel horizontally. The atmosphere acts as a waveguide trapping much of the acoustic energy Georges and Beasley (1977).

4. But hasn't the use of infrasound for monitoring severe weather been researched since the 1970's with no operational uses resulting?

Most past observations used acoustic passbands much lower in frequency than the 0.5- to 5-Hz frequency range currently focused on. There are significant differences between the infrasonic measurement systems applied in the 1970's and 1980's as a part of a global observing network and the higher frequency near infrasound systems now in use. Several features of the global observing system (including the array dimensions, the spatial filter, and the sensor itself) combined to limit the high frequency response to below 0.5 Hz. The severe weather-related infrasound reported in the literature from the historic global infrasonic network involves sound two orders in magnitude longer in wavelength than the newer system and at continental scales of 1000's of kilometers (e.g. Bowman and Bedard, 1971, Georges and Greene, 1975). In contrast, the near infrasound system used to take the current measurements outlined here focuses on frequencies in the range .5 to 10 Hz and regional range scales of 100's of kilometers or less. Table 1 summarizes the differences between these systems. In addition, the processes producing infrasound at extremely low frequencies are certainly quite different than those directly related to tornadoes.

Table 1. Contrasting properties of the infrasound global network and current near infrasound observing systems

System	Typical Sensor Spacings	Spatial Filter Type	Typical Acoustic Wavelengths	Maximum HF Response
Historical Global Infrasound Observing System	10 Kilometers	1000 linear feet	3 to 30 kilometers	.5 Hz
Current Near-Infrasound Observing System	<100 meters	50 feet in diameter	30 to 300 meters	>20 Hz

5. A Typical Infrasonic Summer Day

To provide a reference point for the cases to be discussed in the following section, a recent data set was chosen as being representative of a typical summer day with no notable regional severe weather-related sound present. This provides examples of the infrasonic background in the absence of regional severe weather and should help with interpretation of the case studies. A sequence of plots is presented covering key segments of the local mountain daylight time day: midnight to 6am(0600 to 1200 UTC), 6am to noon(1200 to 1800 UTC), noon to 6pm(1800 to 2400 UTC), and 6pm to midnight(0000 to 0600 UTC on the following day). The 1 to 5 Hz passband chosen for this example most frequently detects infrasonic signals associated with tornadoes.

The midnight to 6am period is often characterized by low correlation coefficients and very weak signals from very distant severe weather (often at ranges > 1000 kilometers). These signals typically are barely above the noise level and would not mask stronger signals from regional tornadic storms. Figure 1 shows plots of data for correlation coefficient, azimuth, and horizontal phase speed for the 6-hour period. The correlation coefficient, R , is related to the signal-to-noise ratio, S/N , with a value of $R=0.5$ corresponding to $S/N=1$. A value of $R=0.3$ corresponds to random noise and good quality signals often have $R>0.9$. The data points on the figure are the maximum correlation coefficient for each 12.8-second processing interval. For each processing interval an array of four sensors is cross-correlated (“beamsteered”) covering all azimuth angles and phase speeds (equivalent to elevation angle). Thus, for the hemisphere around the array contours of correlation coefficient are created and the maximum value R identified. The

azimuth, and phase speed associated with each maximum correlation point are used in making the companion plots in Figure 1.

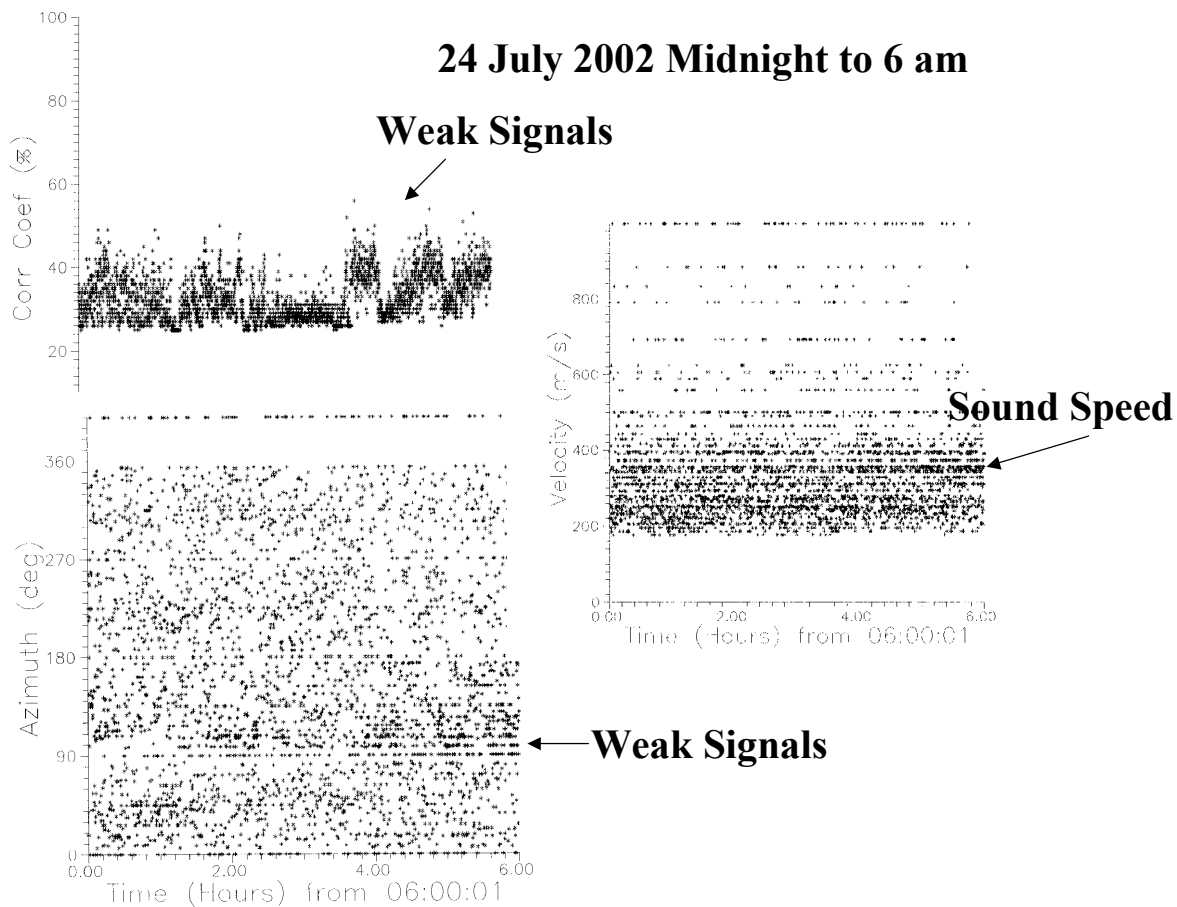


Figure 1. Plots of correlation coefficient, azimuth, and phase speed as a function of time for a 6-hour period starting at 0600 UTC or local midnight

Most values of correlation coefficient on the plot are quite low (most values are between 0.3 and 0.4) with a few spikes going to higher values. There are three surges near the end of the interval with values consistently above 0.4. The plot showing azimuth values is for the most part a random scatter of data points consistent with random noise. Periodically more consistent directions are evident corresponding to regions of increased correlation coefficient. This is clearest near the end of the period. The phase speed plot shows a high degree of scatter with points close to the speed of sound appearing most consistently near the end of the interval when the larger correlation coefficient values occurred. The azimuth direction from the east southeast probably originated from severe weather in the Alabama area as indicated by Nexrad mosaic imagery.

Figure 2 shows plots of correlation coefficient and azimuth data for the 6am to 12 noon interval. This period often shows short impulsive signals from civilization events (e.g. quarry blasting), which can be easily distinguished from natural sound generation mechanisms. The

correlation coefficient plot shows some small impulsive signals, but most points are merely random noise. These impulses could be examined more closely with reprocessing. For example the data could be simply re-plotted with only those data points with values of $R > 0.45$ shown. The azimuth plot shows essentially a scatter plot with the remnants of the weak signals near the end of Figure 1 continuing for about an hour.

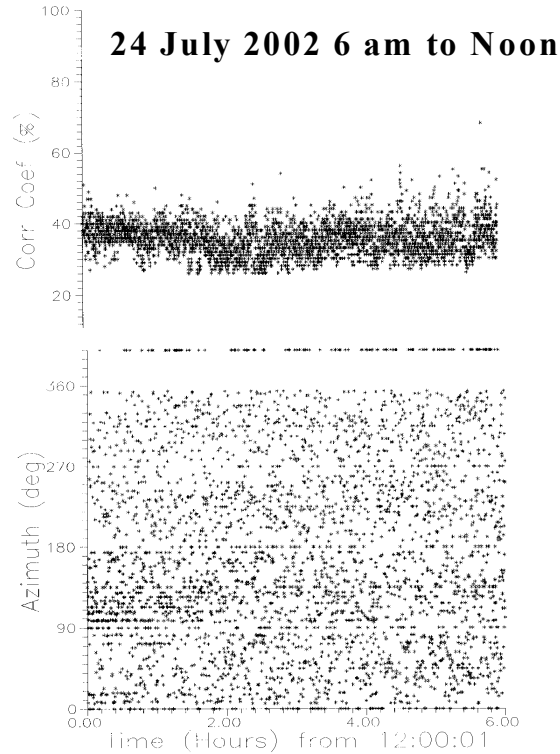


Figure 2. Plots of correlation coefficient and azimuth as a function of time for a 6-hour period starting at 1200 UTC or 6am local time.

On this day there was no significant regional weather occurring and Figure 3 covering from noon to 6pm again shows mostly random noise with some impulsive data points and a weak tendency for sporadic segments of more consistent azimuth measurements. For the front range region of Colorado this period can be the most active part of the day with storms moving from the foothills to the east. Also, as the day progresses storms produced to the north along the Cheyenne Ridge or to the south along the Palmer Divide can produce outflow boundaries. These can collide and produce new convection. This particular interval is quiet with weak convective activity and would be considered as not very interesting.

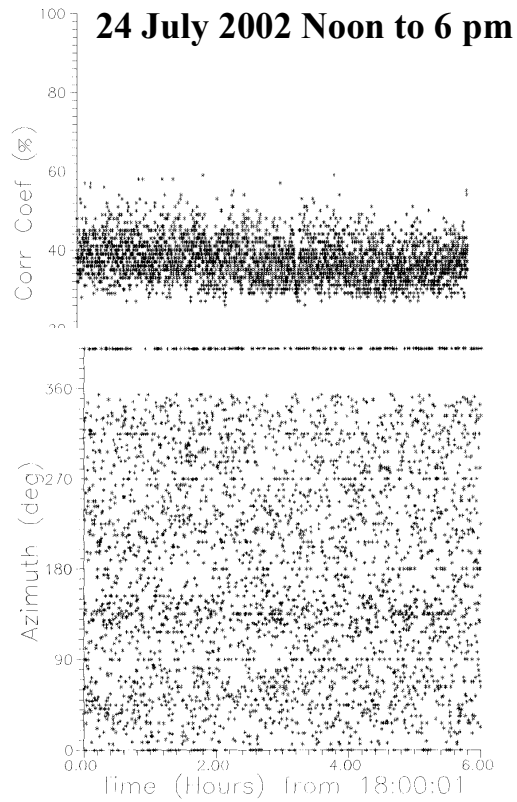


Figure 3. Plot of correlation coefficient and azimuth as a function of time for a 6-hour period starting at 1800 UTC or noon local time.

The interval from 6pm to midnight (Figure 4) continues this trend containing mostly random noise mixed with some weak, low quality signals probably from distant sources. Often during this time period severe weather will move to the east and become more intense. Storms in Nebraska, Kansas, and Oklahoma can contribute to the infrasonic background.

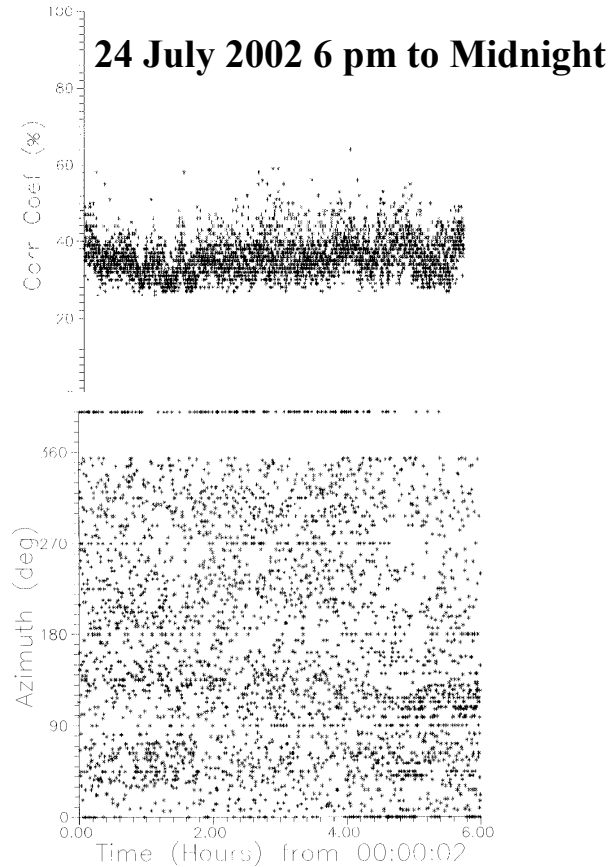


Figure 4. Plot of correlation coefficient and azimuth as a function of time for a 6-hour period starting at 0000 UTC or 6pm local time.

6. A contrast to the quiet summer day

At 0100 UTC on 6 July 2000 Nexrad imagery showed an echo in southwest Nebraska moving to the south southeast. Infrasound increased abruptly from a NNE direction at about 0140 UTC and continued at high signal-to-noise ratios until about 0320 UTC. Sporadic acoustic signals continued until after 0400 UTC. The tornado hit near Dailey, Colorado at 0310 UTC, 1-hour and 30 minutes after the first infrasonic signal detection causing 2 injuries and $\frac{3}{4}$ million dollars in damage. Figure 5 shows the large increase in correlation coefficient associated with this tornadic storm and Figure 6 shows the progressive azimuth shift that occurred.

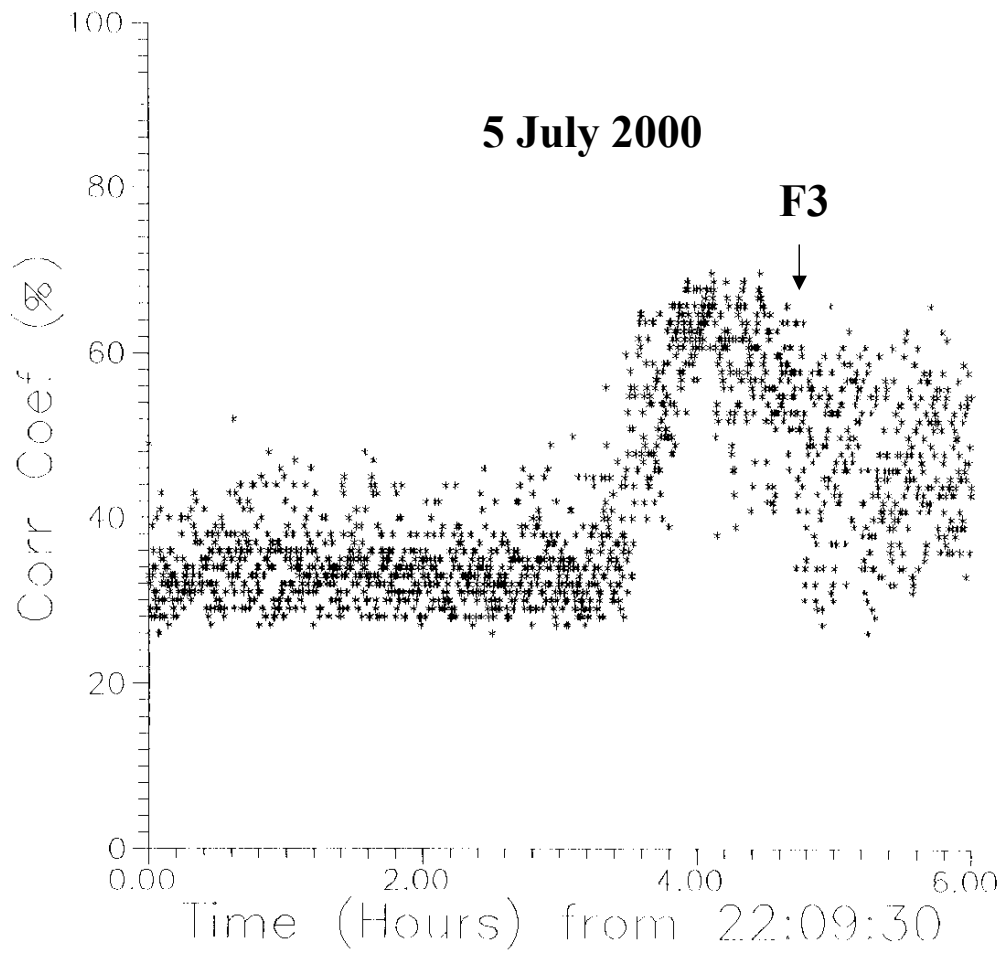


Figure 5. Plot of correlation coefficient as a function of time for a six-hour period starting at 2209:30 UTC. The time of the F3 tornado report is indicated on the plot by an arrow.

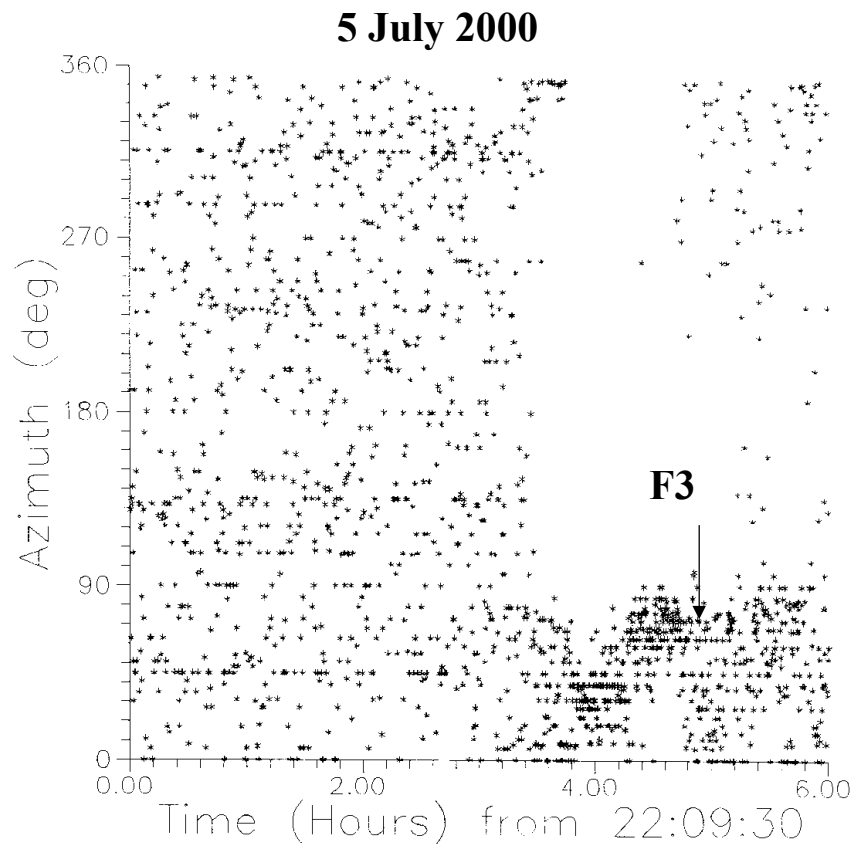


Figure 6. Plot of azimuth as a function of time for a six-hour period starting at 2209:30 UTC. The time of the F3 tornado report is indicated on the plot by an arrow. The point of the arrow indicated the azimuth to Dailey, Colorado.

7. How can vortices generate sound?

There are a number of possible ways tornadoes and other vortices can generate sound. The conceptual view shown in Figure 7 indicates some possibilities, including shear instabilities, boundary layer sound, fluid instabilities (e.g. core bursting), and the radial modes of vibration of the vortex core.

VORTEX SOUND GENERATION

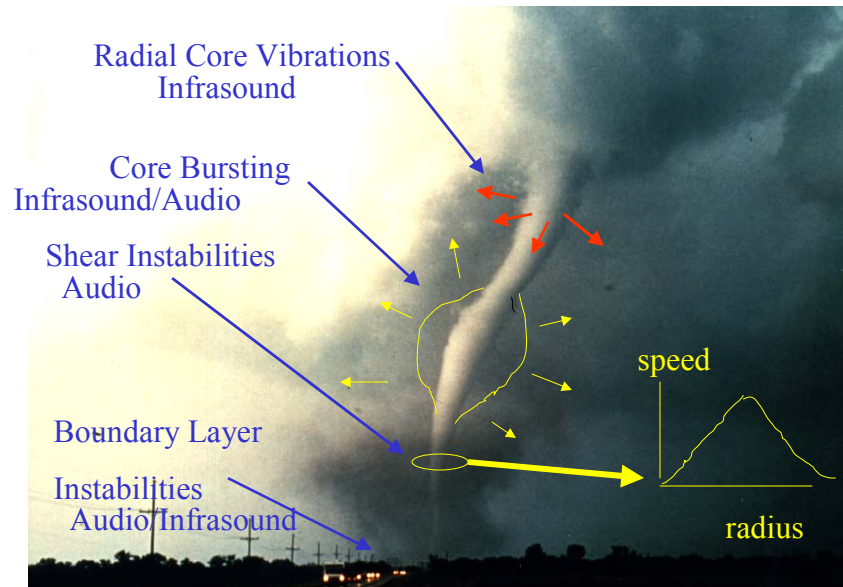


Figure 7. Conceptual view of vortex sound generation mechanisms.

Bedard (2002) contrasts some of these possibilities with measurements associated with tornadoes, finding the radial vibration model (Abdullah, 1966) is most consistent with the infrasonic data. This model predicts that the fundamental frequency of radial vibration will be inversely proportional to the core radius. A radius of about 200 m will produce a frequency of 1 Hz.

8. Case studies of infrasound associated with tornadoes and tornadic storms

As indicated in section 4 infrasonic systems developed by the Environmental Technology Laboratory and operating at higher frequencies (near 1 Hz) than historical systems have provided a new view of severe weather acoustics. This has led to evidence that infrasonic observatories can help address NWS goals to improve tornado warning lead times. A series of case studies review observations of low frequency sounds from tornadic storms, indicating a number of detection scenarios and potential warning times. The evidence is that long-lived, concentrated vortices may be a common feature of some tornado producing storm types and their detection may serve as a basis for improving warnings. A series of papers submitted to journals and in progress discuss the details of these and other cases.

1. Case of 6 June 1995 (Bedard,2002)- A vertically concentrated vortex aloft eventually descended to the surface. Sound was detected and tracked aloft 30 minutes before the vortex reached the surface and a tornado reported. The downdraft was probably relatively weak and

larger than the vortex causing downward advection but not stretching. The vortex appeared sporadically on Doppler radar until touchdown.

1. Case of 31 May 1998, Spenser, SD tornado (Bedard et al., 2002)- A continuous vortex measured by Doppler on Wheels (Wurman, 1999) was periodically reported as a series of individual tornadoes because of variations in visibility and damage paths. After infrasound first detected the vortex (corrected for sound travel time since the distance was about 800 kilometers), the circulation produced 8 tornado reports on a path over the next hour and 25 minutes. Thirty-eight minutes elapsed before an F4 tornado struck Spenser, SD. The figure below is a DOW image of the evolving vortex.

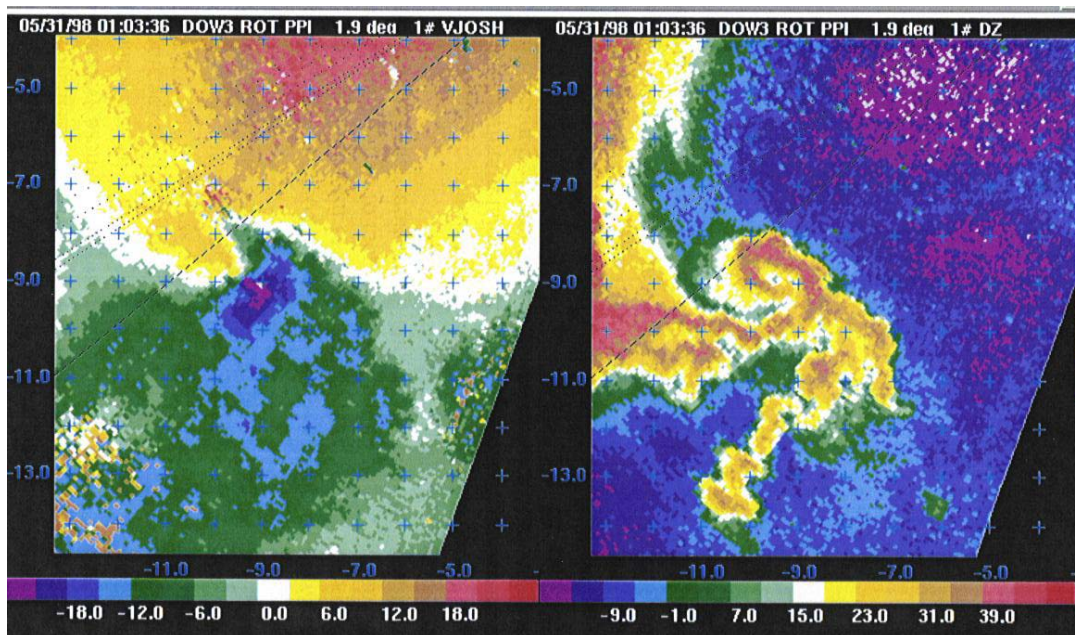


Figure 8. Doppler radar images of radial velocity and reflectivity at 0103:36 UTC, showing the evolving tornado (with the permission of J.Wurman).

2. Case of 28 June 1999 cyclic production of tornadoes(Bedard et al., 2002)- - At 0330 UTC infrasound was first detected from the storm system. Over the next 3 hours three tornadoes were reported as the system moved SSE continuously radiating infrasound. The first reported tornado was about 1-hour after sound was first detected. The figure below is a plot of infrasonic azimuth as a function of time clearly showing the movement of the system. The arrows indicate the times of reported tornadoes with the points of the arrows indicating the azimuth to the tornado location.

28 June 1999

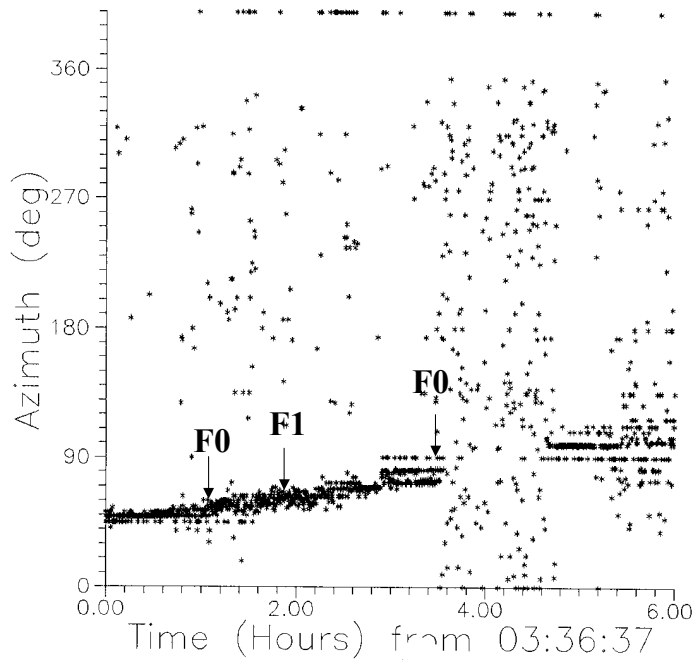


Figure 9. Plot of azimuth of arrival of the infrasound as a function of time for a six-hour period starting at 0336 UTC. The arrows indicate the times of tornado observations with the tips of the arrows identifying the expected azimuth of arrival.

3. Case of 15 June 1997(Bedard et al., 2002)- - Infrasonic signals occurred at 2111 UTC initially at high elevation angles. Ten minutes later a tornado was reported within 3 kilometers of the observatory in the direction from which sound was originating. The vortex was originally aloft and then probably stretched downward until reaching the surface. The photo below shows the tornado tapering toward the ground where it produced a damage path 50 yards wide.

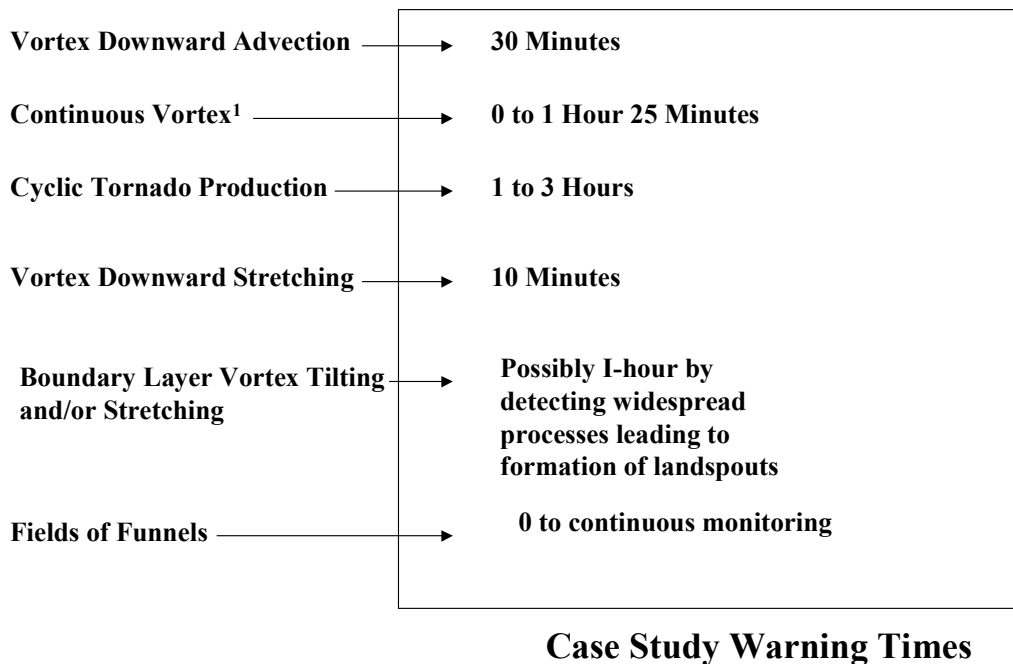


Figure 10. Photo of the tornado taken by police officer David Osborne and reproduced here with his permission.

4. “Landspout” scenario(Bedard et al., 2002)- - The production of landspouts by boundary layer vortex tilting and/or stretching is a process that potentially can occur over a fairly broad area (e.g. Szoke, 1991, Wilson, 1986). We have detected multiple regions generating sound before and after reports of tornadoes. It is possible that only a fraction of those areas with the potential to produce tornadoes actually do so. Possibly could detect the evolutionary process as an updraft stretches and/or tilts the vortex. Well-documented cases remain to be obtained with remote sensor information.
5. Long-lived fields of short-lived funnels on 27 August 1997 (Bedard and Bloemker, 2002)- Visual observations and photographs were taken of funnels almost directly overhead while infrasound was being detected from aloft. The sound occurred sporadically over a period of about one-hour, while both vertically and horizontally oriented vortices periodically appeared. These were high based funnels (e.g. Bluestein, 1994) and did not produce tornadoes.

To place these measurements in context we examined acoustic data for two significant large hail-producing storms studied by Doppler radar, chase teams, and aircraft. The storms showed no evidence of vortices and no infrasound occurred. This indicates that the radiation of infrasound is not a natural consequence of all severe weather.

The case studies summarized above indicate that infrasound is radiated by atmospheric vortices at times restricted to limited vertical heights within storms. Also, some tornadic storms produce sound continuously for durations of hours, periodically producing tornado reports. The figure below summarizes case study warning times. For a cyclic tornado-producing storm that is continuously radiating infrasound, we have no way to indicate when a vortex will reach the surface, but rather indicate the potential for tornado production. An assumption is that the observing site is regionally located so that acoustic delay times are not significant (< several minutes). Figure 11 summarizes detection scenarios indicating potential warning times that could be provided. Realizing that just a modest set of cases provide no statistical numbers and can only indicate potential, it is still worthwhile to summarize the value in terms of possible warning times for these specific events. To the extent that they are representative of the majority of tornado producing processes can only be evaluated with network experience.



1 A presumption is that sound was not generated until a coherent vortex had evolved

Figure 11. Summary of case study potential warning times.

Figure

9. But are there regional signals that can cause false alarms?

As indicated in section 5, typical infrasonic days in the summer (and also the spring) at the Boulder Atmospheric Observatory (BAO) infrasonic observatory east of Boulder, CO are usually free from signals that could mask severe weather signals or cause false alarms. However, we expect each regional infrasonic observatory will have a background of signals that can be systematically collected and characterized. At the BAO there is an unusual signal that occurs almost daily during the summer months. It comes from an east northeast direction and probably originates in Nebraska. The signal usually arrives about 1500 UTC (9am MDT) and usually lasts about 15 minutes. It must involve the release of significant energy, possibly by an industrial process.

Paradoxically, such a signal (occurring outside of the strong convective time of day) can be useful as a system check or for propagation studies. In this section this signal is used to show an example of the data visualization options under development. A survey of the infrasonic background is an effort that will help greatly with data interpretation.

Also, we have found a close association between infrasound and sprites and plan a paper on this work. Indications are that this type of infrasonic signal is short and impulsive in the region of the source. A paper by Bedard and Carnathan (2002) addresses such complicating factors.

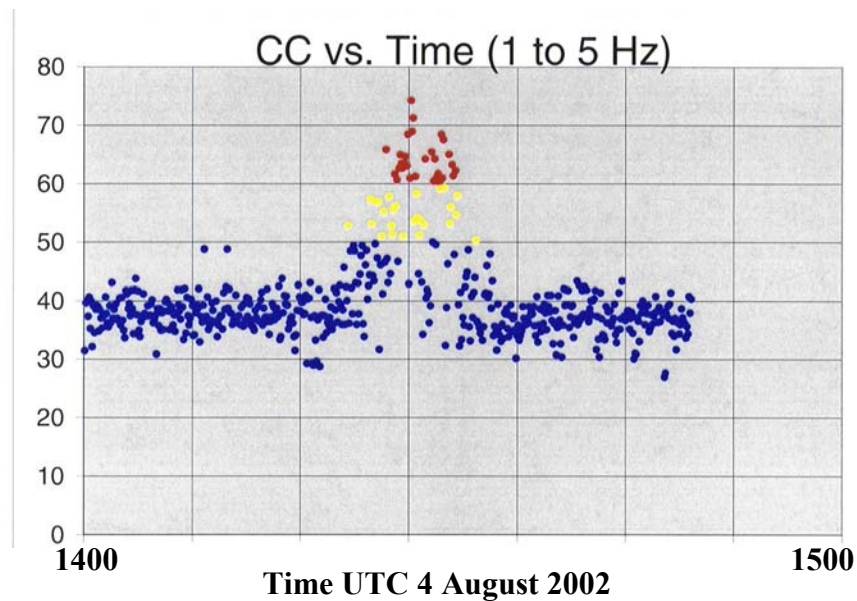


Figure 12. Correlation coefficient as a function of time for a 1-hour interval showing the features of the recurring regional signal that is not related to severe weather. The data points are color coded with correlation coefficients > 0.6 in red and points > 0.5 yellow.

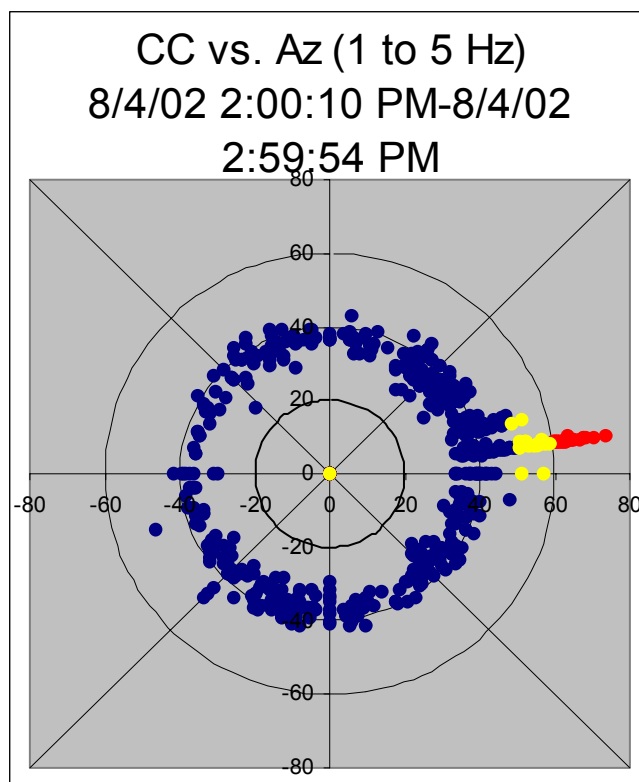


Figure 13. Polar plot of signal azimuth data between 1400 and 1500 UTC on 4 August 03 showing the signal from the east northeast. The data points are color coded with correlation coefficients > 0.6 in red and points > 0.5 yellow.

10. How can infrasonic observatories improve tornado warnings?

1. Provide vortex detection capabilities where radar constraints exist (e.g. obstacle blocking, longer ranges where radar resolution is degraded, short ranges where high elevation radar scans are limited).
2. Provide detection continuity between radar scans (The interval between consecutive Nexrad volume scans is 5 minutes).
3. Provide information on smaller diameter vortices.
4. Provide information on vortices of limited vertical extent, which may not show clearly on volume scan displays.
5. Potentially provide guidance for optimizing radar scans.
6. Provide information on vortex core size (using the sound generation model of Abdullah, 1966).

11. What are the next steps?

Plans include continuing to document the results of measurements and analyses, as well as improving detection hardware and software. Our goal is to work closely with our sister labs (NSSL and FSL) and the NWS as we move toward implementation of a prototype demonstration network. We will also work with other organizations such as FEMA. There is also the potential that other missions for infrasound observing systems (such as sprite research or the International Monitoring System of the Nuclear Test Ban Treaty) could help accelerate development. We will be sensitive to these opportunities for support. We will also make every effort to include other NOAA-supported technologies (e.g. seismic electromagnetic, and pressure sensors) in evaluation programs. Specifically, we plan to complete analyses of the data obtained during the summers of 2000, 2001 and 2002, evaluate the effectiveness of visualization software, and present and publish these results.

1. Execute a prototype network experiment to demonstrate and further evaluate the potential of infrasonic detection systems to improve tornado warnings.
2. Include infrasonic systems in experiments designed to study tornadic storm dynamics so that data sets permitting collaborative analysis are available
3. Perform 3-D ray trace studies to define the effects of a variety of atmospheric refractive structures on propagation and detection.
4. Perform comparisons between infrasound detected from tornadoes and fully compressible model results.
5. Continue to explore the lessons that can be learned from archived data for infrasound related to tornadoes, as well as possible sources of noise and false alarms (e.g. Bedard and Carnathan, 2002).
6. Access infrasonic data in real time and make this information available to researchers and NWS forecasters.

12. What form will the prototype network take? –and- What steps will be critical to assessment?

The array will make use of one existing infrasonic array at the Boulder Atmospheric Observatory, east of Boulder, Colorado. We have operated at the site for a number of years and know the background of signals types and their statistics quite well. A Goodland, Kansas site will be ideal because we have operated there during the STEPS campaign during the summer of 2000 and have some background on the infrasonic signal environment. This location together with the BAO provides a good baseline for triangulation to the north and south. A site at Pueblo, Colorado provides a baseline for triangulation in eastern Colorado as well as the foothills and

near mountains to the west. The locations are logistically attractive because we can visit the more distant sites in a single day by vehicle. We will make every effort to locate near WSR-88D radars to provide the best possible data sets for comparison. Figure 14 is a map of the prototype network with the simulation of a triangulation on an infrasonic source in east central Colorado.

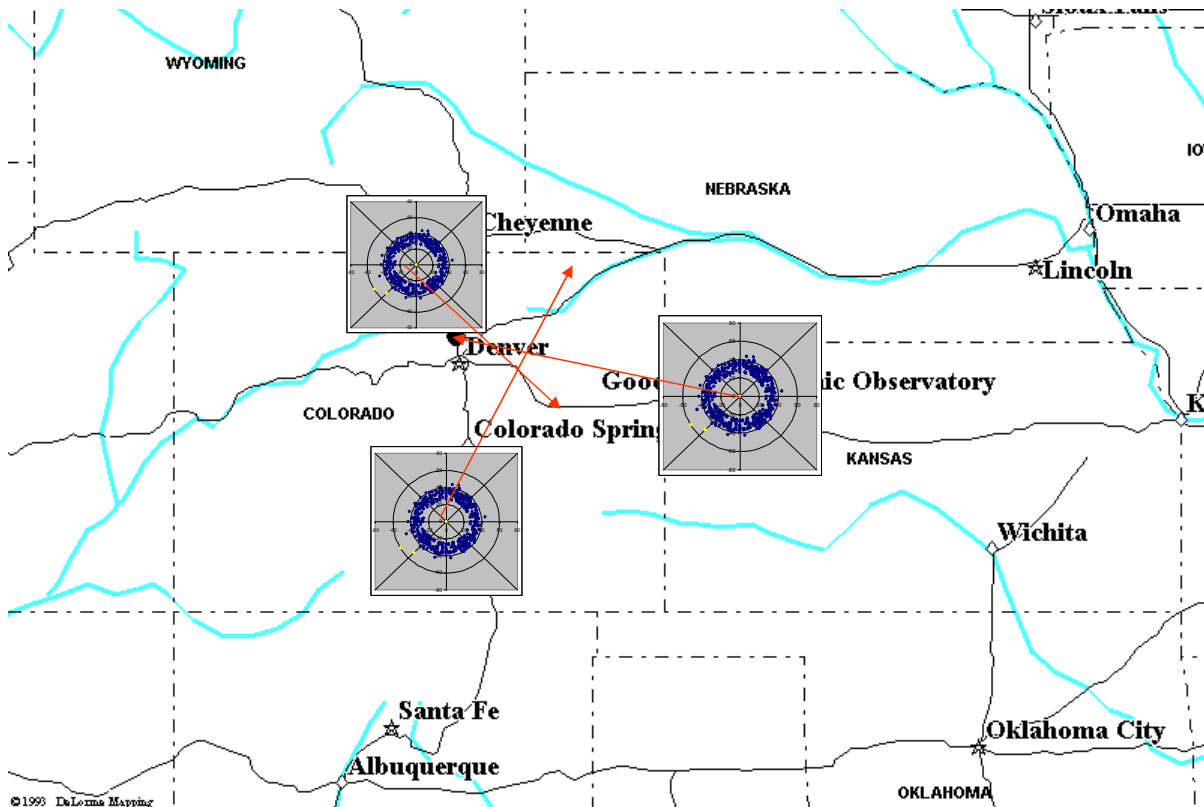


Figure 14. Map of 3-station prototype demonstration network in eastern Colorado and Kansas showing a simulated signal detection in east central Colorado derived from polar plots.

SIGNIFICANT MILESTONES/ACTIVITIES/SCHEDULE:

1. Complete series of papers documenting detection of infrasound from tornadoes and the acoustic radiation processes (Spring 2003).
2. Develop detailed field deployment plan for infrasound network demonstration (October 2002).

3. Test proposed eddy dissipation techniques to reduce wind pressure noise (Winter 2003).
4. Set up and operate an infrasonic network during the spring and summer of 2003 that provides user-oriented real-time display of processed data on infrasound source and location at a central data analysis site (May2003).
5. Make data widely available to collaborating researchers and forecasters (June 2003).
6. Work with numerical modelers to apply fully compressible numerical models to study vortex sound generation processes (June 2003).
7. Participate in field experiments to expand the number of infrasonic case studies that can be compared with remote sensor data sets (June 2003).
8. Document the experiences and recommendations of researchers and forecasters, concerning the use of real-time infrasonic data for tornado detection and warning (Fall 2003).

13. What are the Anticipated Benefits-to-Cost Ratios?

From the document “National Weather Services Research And Development Needs and Priorities” the 2001 lead time goal was 12 minutes with the actual performance 10 minutes. By 2008 the tornado lead time goal increases to 15 minutes as shown in the figure below.

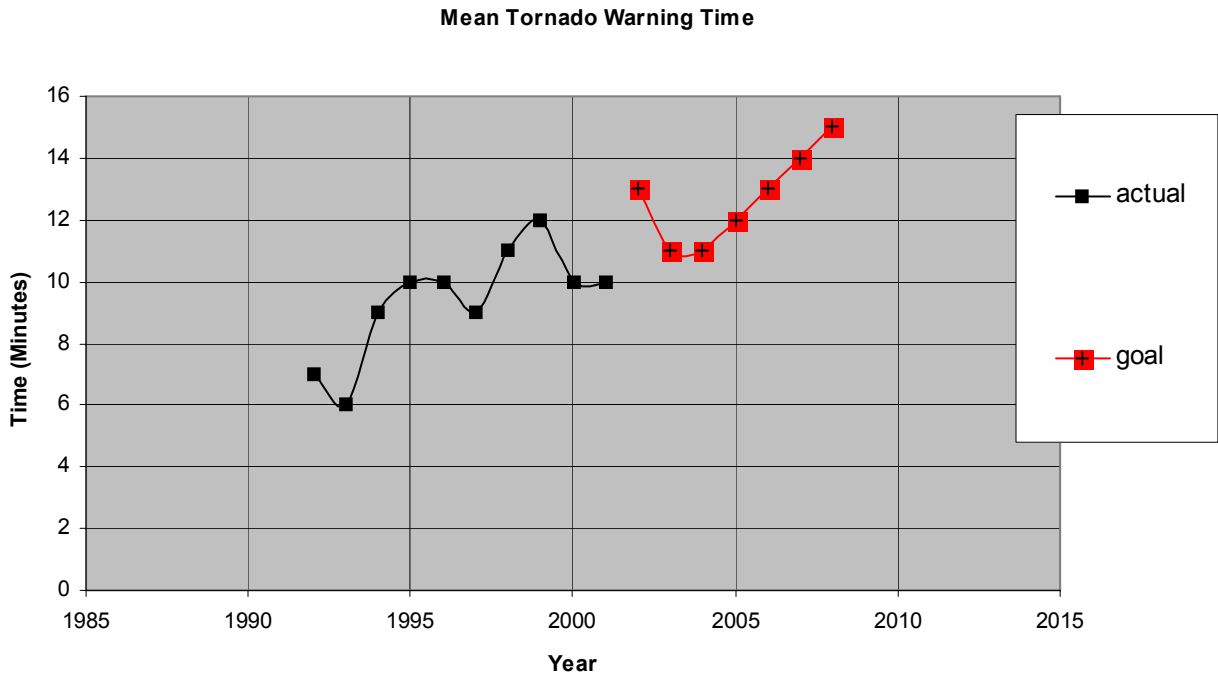


Figure 15. Mean tornado warning time as a function of year contrasting the mean warning times actually achieved with the goals. This figure was re-plotted from the document “National Weather Service Needs and Priorities”.

For some of the case study situations outlined, infrasonic systems have the potential to directly respond to the NWS goals to improve warnings. A network of infrasonic systems should also improve tornado probability of detection and help reduce false alarms.

A recent paper by Pielke and Carbone (2002) updates the impacts of tornadoes on loss of life and damage costs. The annual mean loss of life from tornadoes is 56 and the mean annual dollar loss is 777 million. The National Climatic Data Center reported for 1999 94 fatalities, 1824 injuries, and 1.9 billion dollars in damage.

We estimate the cost of the hardware for a single infrasonic observing system as <\$50,000. Our vision is that these systems will be ideally located at Nexrad sites, making use of existing logistics and data transfer systems where possible. During the recent STEPS experiment we were able to temporarily install an infrasonic system at the NWS site in Goodland, Kansas near the WSR-88D. Using the case studies as examples, the warning times range from zero (for a tornado evolving at the surface before sound is radiated) to over one-hour (for a cyclic tornadic storm). The possible warning time to infrasonic system cost ratios range from 0 to about 1-minute per \$1000 of cost. It is difficult to imagine significant reduction of property damage even with a lead time goal of better than 15 minutes achieved. On the other hand, there should be a significant impact on loss-of-life and injury statistics.

Current efforts are to document results of infrasonic detection of tornadoes as promptly as possible in the formal literature and also develop statistics for probabilities of detection and potential sources of false alarms and noise. The system should be highly complementary to WSR-88D since in addition to infrasound potentially filling gaps in radar detection, the radar in turn can limit acoustic false alarms from sound sources that are not weather-related.

This technology is at the ideal point for demonstration in an operational context. Most major issues have been identified and addressed.

14. References

Abdullah, A. J., 1966: The "musical" sound emitted by a tornado. *Mon. Wea. Rev.*, **6**, 213–220.

Bedard, A.J., Jr. and T.M.Georges, 2000: Atmospheric infrasound. *Physics Today*, March, 32-37.

Bedard, A.J., Jr., 2002: Low-frequency atmospheric acoustic energy associated with vortices produced by thunderstorms (submitted to *Mon. Wea. Rev.*).

Bedard, A.J. Jr., R. Bloemker, and J. Carnathan, 2002: Infrasound from Tornadoes and Tornadic Storms: Part 1 Case studies illustrating various detection scenarios (to be submitted to *J. Applied Meteorol.*)

Bedard, A.J. Jr., and J. Carnathan, 2002: Infrasound from Tornadoes and Tornadic Storms: Part 2 Case studies illustrating factors complicating detection (to be submitted to *J. Applied Meteorol.*).

Bluestein, H.B., 1994: High-based funnel clouds in the southern plains. *Mon. Wea. Rev.*, **122**, 2631-2638.

Bowman, H. S., and A. J. Bedard, Jr., 1971: Observations of infrasound and subsonic disturbances related to severe weather. *Geophys. J. Roy. Astr. Soc.*, **26**, 215–242.

Brady, R.H. and E.J. Szoke, 1989: A case study of nonmesocyclone tornado development in northeast Colorado: Similarities to waterspout formation. *Mon. Wea. Rev.*, **117**, 843-856.

Cook, R. K., 1962: Strange Sounds in the Atmosphere, Part 1, Sound 1

Daniels, F. B. 1959: Noise reducing line microphone for frequencies below 1 Hz, *J. Acoust. Soc. Amer.*, 31.

Georges, T. M., and G. E. Greene, 1975: Infrasound from convective storms: Part IV. Is it useful for warning? *J. Appl. Meteor.*, 14, 1303–1316.

Georges, T. M., and W.H.Beasley, 1977: Infrasound refraction by winds. *J. Acoust. Soc. Amer.*, 61, 28-34.

Pielke, R. Jr., and R.E.Carbone, 2002: Weather impacts, forecasts, and policy. *Bull. Amer. Meteorol. Soc.*, 83, , 393-403.

Szoke, E.J., 1991: Eye of the Denver Cyclone. *Mon. Wea. Rev.*, **119**, 1283-1292.

Wilson, J.W., 1986: Tornadogenesis by nonprecipitation induced wind shear lines. *Mon. Wea. Rev.*, **114**, 270-284.

Wurman, J., 1999: Preliminary results from the radar observations of tornadoes and thunderstorms experiment (ROTATE-98/99) *Proc. 29th International Conf. On Radar Meteorol.*, 12-16 July, Montreal, Quebec, Canada, 613-616.